JOURNAL OF MASS SPECTROMETRY
J. Mass Spectrom. **33**, 705–712 (1998)

Characterization of β-lactams by Photodissociation and Collision-activated Dissociation in a Quadrupole Ion Trap

Brian J. Goolsby and Jennifer S. Brodbelt*
Department of Chemistry and Biochemistry, The University of Texas at Austin, Austin, Texas 78712 USA

Electrospray ionization was used to introduce β-lactams, including cephalosporin and penicillin analogs, into a quadrupole ion trap for analysis by collision-activated dissociation (CAD) and infrared multiphoton dissociation (IRMPD). The two dissociation methods provided similar spectra; however, photodissociation requires substantially less tuning than is typically required to optimize CAD. Moreover, IRMPD was effective even at the elevated pressures introduced by the electrospray source. Both CAD and IRMPD promote cleavage across the β-lactam ring, resulting in highly diagnostic fragmentation patterns. Time-resolved and SWIFT methods were used to determine fragmentation genealogies of the ions created by IRMPD. © 1998 John Wiley & Sons, Ltd.

KEYWORDS: photodissociation; collision-activated dissociation; β-lactams; ion trap; SWIFT

INTRODUCTION

The discovery, evaluation and comparison of various dissociation techniques have been key issues in making mass spectrometry the powerful analytical technique that it is today. Factors involved in choosing an appropriate dissociation method include ease of implementation and use, applicability to specific analytes and selectivity for specific mass/charge ratio. Advances in matrix-assisted laser desorption/ionization (MALDI) and electrospray technology have allowed the production of ions from large biomolecules, and great effort has been devoted to the development of techniques for the structural elucidation of high-mass ions.[1–3]

Infrared multiphoton dissociation (IRMPD) is a technique that is gaining acceptance as a versatile method for fragmentation of both small and large ions. McLafferty and co-workers[4] used IRMPD to fragment proteins as large as 29 kDa in a Fourier transform ion cyclotron resonance mass spectrometer. This method was useful for determining protein structure, and the PD method compared favorably with collisional-activated dissociation (CAD) with respect to efficiency of fragmentation and reduction in ion losses from scattering or other collisional effects. Yost and co-workers[1] compared CAD and PD for the analysis of several classes of compounds, including oligosaccharides, ribonucleic acid dimers and peptides, in the quadrupole ion trap. They found that using mirrors to pass the laser beam repeatedly through the trapped ion cloud increased the photodissociation efficiency. Russell and co-workers[5] used 6.4 eV photons from an excimer laser to dissociate peptides as large as 14 kDa in a time-of-flight instrument. Much higher energy photons were required because the time-of-flight time-scale was not sufficient for absorption of multiple photons. Hence it is arguably simpler to implement photodissociation in one of the trapping spectrometers because of the ability to store ions for long periods, thus allowing multiphoton absorption. IRMPD has also been used in conjunction with quadrupole ion trap mass spectrometry for the dissociation of small biomolecules and metal ion–crown ether complexes.[6] Here again, it was found that the fragments provided a wealth of structural information.

Because of the different manner in which energy is deposited into analyte molecules, IRMPD has several advantages over collision-based dissociation methods. For instance, photoabsorption does not disrupt the path of an ion or cause scattering. Nearly every type of organic bond can absorb photons of infrared wavelengths, and the total energy deposited may be controlled by attenuating the laser power or irradiation time. Another difference between IRMPD and CAD is that low-energy collisions with bath gases may inhibit photodissociation by damping excited vibrational modes through collisional deactivation, whereas collisions are essential to the CAD mode. Because the rate of energy loss due to collisions can equal or exceed the rate of energy deposition by photon absorption, dissociation may not occur when IRMPD is undertaken in higher pressure environments.[5] However, increasing the photon flux can overcome this problem. Overall, the

* *Correspondence to*: J. S. Brodbelt, Department of Chemistry and Biochemistry, The University of Texas at Austin, Austin, Texas 78712, USA
E-mail: jbrodbelt@mail.utexas.edu
Contract/grant sponsor: National Science Foundation; Contract/grant number: CHE-9357422; Contract/grant number: CHE-9421447.
Contract/grant sponsor: Robert A. Welch Foundation; Contract/grant number: F1155.
Contract/grant sponsor: Texas Advanced Research Program.
Contract/grant sponsor: Dreyfus Foundation.

CCC 1076–5174/98/080705–08 $17.50

Received 15 January 1998
Accepted 14 April 1998

potential advantages of IRMPD, especially in the context of the structural elucidation of large biomolecules, have prompted further investigation of the method.

β-lactams represent a large group of antibiotic pharmaceuticals, both in application and in volume of production.[7] Over the past few decades, numerous structural variations have been incorporated in attempts to find more potent, more stable compounds that are effective against penicillin-resistant bacteria. Mass spectrometry has played a crucial role in the evolution of β-lactams,[8] and these compounds provide an interesting array for a comprehensive and comparative dissociation study, as described here (Fig. 1).

Numerous groups have previously studied β-lactams using various mass spectrometric techniques. Earlier work included chemical ionization (CI) with isobutane and pyrolysis ionization, both of which resulted in characteristic fragments but lacked operator control over the extent of dissociation.[9,10] Since the early 1980s, several groups have evaluated ionization techniques such as CI, fast atom bombardment (FAB) and electrospray ionization (ESI) for β-lactam analysis, and while a few groups incorporated tandem mass spectrometry, the majority relied on spontaneous fragmentation.[11–16] Upon dissociation, fragmentation was found to occur predominately across the lactam ring.[9,11–16] The objective of the present study was the comparison of IRMPD and CAD for the structural characterization of a group of β-lactams. Analytical factors including dissociation efficiencies, tunability and the ability to map fragment genealogies were evaluated.

EXPERIMENTAL

Experiments were performed on an electrospray ionization instrument with an interface modeled after the Oak

Cephalosporin Analogs

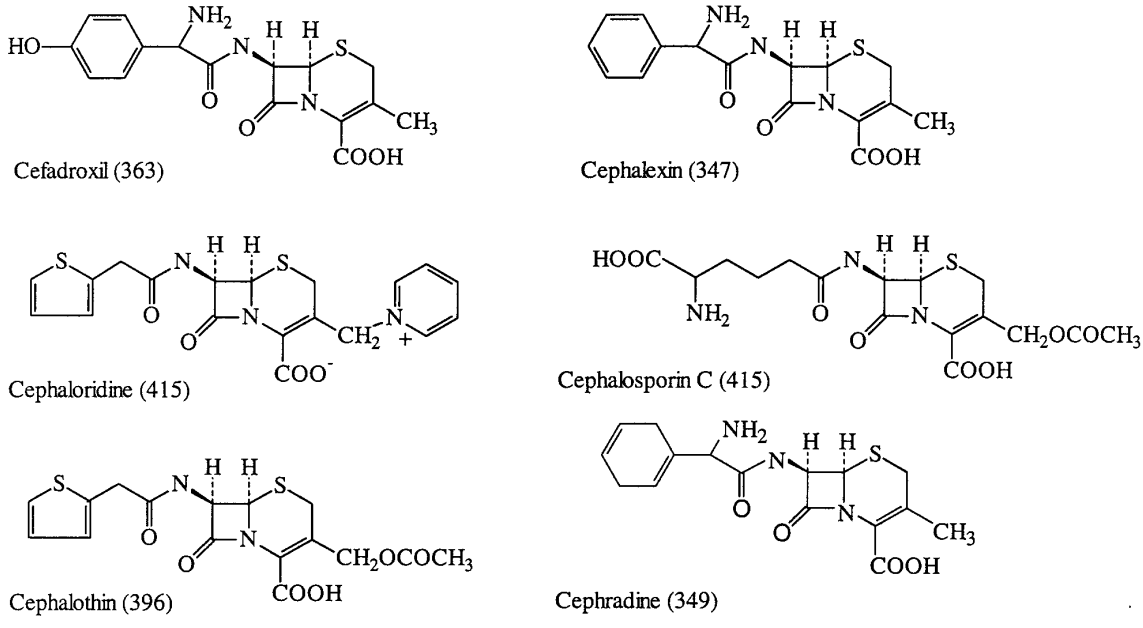

Penicillin Analogs

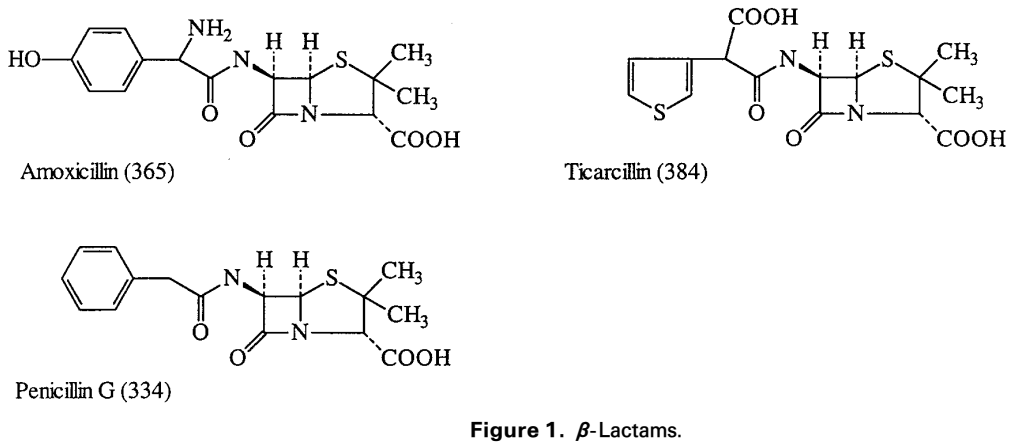

Figure 1. β-Lactams.

Table 1. Comparison of major fragments from CAD and PD[a]

β-Lactam	PD	CAD
[Amoxicillin + H]$^+$	−17 (90%)	−17 (30%)
366	−159 (<5%)	−159 (20%)
	−206 (<5%)	−206 (20%)
	−252 (<1%)	−252 (30%)
[penicillin G, K salt + H]$^+$		−17 (15%)
373	−159 (20%)	−159 (30%)
	−175 (5%)	−175 (15%)
	−213 (25%)	−213 (30%)
	−259 (50%)	−259 (10%)
[ticarcillin, Na salt + H]$^+$	−44 (5%)	−44 (15%)
407	−72 (<1%)	−72 (10%)
	−203 (35%)	−203 (35%)
	−220 (20%)	−220 (15%)
	−225 (10%)	−225 (10%)
	−247 (15%)	−247 (5%)
	−293 (15%)	−293 (10%)
[cefadroxil + H]$^+$	−17 (<1%)	−17 (<1%)
364	−156 (45%)	−156 (20%)
	−174 (<1%)	−174 (5%)
	−206 (45%)	−206 (25%)
		−224 (<1%)
	−250 (10%)	−250 (50%)
[cephalexin + H]$^+$	−157 (5%)	−157 (5%)
348		−174 (5%)
	−190 (85%)	−190 (75%)
		−208 (10%)
	−242 (10%)	−242 (5%)
[cephaloridine + H]$^+$	−79 (<5%)	−79 (<5%)
416	−258 (<5%)	−258 (<5%)
	−264 (<5%)	−264 (15%)
		−292 (<5%)
	−336 (90%)	−336 (80%)
[cephalosporin *c* + H]$^+$	−60 (<1%)	−60 (10%)
416	−104 (40%)	−104 (45%)
	−150 (10%)	−150 (<1%)
	−272 (50%)	−272 (35%)
		−319 (10%)
[cephalothin, Na salt + H]$^+$	−60 (35%)	−60 (35%)
419	−104 (5%)	−104 (5%)
	−148 (15%)	−148 (5%)
	−217 (20%)	−217 (25%)
	−243 (15%)	−243 (20%)
	−269 (10%)	−269 (10%)
[cephradine + H]$^+$	−157 (<1%)	−157 (5%)
350	−174 (5%)	−174 (25%)
	−192 (90%)	−192 (60%)
		−210 (10%)
	−242 (5%)	−242 (<1%)

[a] CAD parameters: 0.5–2.0 V_{p-p}, 10–30 ms, 1 mTorr. PD parameters: 30 W laser power, 50–100 ms, 0.1 mTorr.

Ridge design.[17] Modified Finnigan ITD electronics and ITMS software allowing TTL triggers were used. An Apollo CO_2 Model 575 CW laser with a variable-speed shutter was used for IRMPD. The laser power was typically 30 W with a 6 mm beam diameter. The PD set-up was described in detail previously.[6] No bath gas was added during PD experiments and the pressure was nominally 1×10^{-4} Torr (1 Torr = 133.3 Pa) (mainly air and methanol) owing to the high background pressure from the ESI interface. Exposure times for experiments comparing PD with CAD ranged from 50 to 100 ms, optimized for appearance of MS/MS ions.

CAD voltages, typically 0.5–2.0 V_{p-p}, were applied to the end-cap electrodes. The chamber pressure was held at 1 mTorr for CAD experiments by addition of He. Either a Finnigan tickle board or a SWIFT apparatus[6] was used to generate the appropriate waveform for dissociation. The SWIFT set-up consisted of a Tektronix AWG2005 arbitrary waveform generator controlled by a desktop computer running National Instrument's LabView software. Isolation was carried out prior to CAD by the SWIFT technique or a simple r.f. ramp to eject low-mass interferences.

Solutions were typically 5×10^{-4} M in methanol containing 1–5% acetic acid. The average flow-rate was 2 μl min^{-1}, generated by a Harvard syringe pump. β-lactams were obtained from Sigma (St Louis, MO, USA) and were used without further purification.

RESULTS AND DISCUSSION

Prior to acquisition of CAD and IRMPD spectra, the ESI parameters were optimized for the production of molecular-type ions. The targeted molecular ions were isolated, then CAD and IRMPD were performed in succession to ensure that the conditions were as similar as possible for the two experiments. For the general comparisons, excitation energy was applied until ~50–75% of the molecular ion peak had disappeared and an ample fragment ion current was observed. This typically required 50–100 ms for the IRMPD spectra and 10–30 ms for the CAD spectra. The abundances of IRMPD fragments are clearly dependent on irradiation time, and spectra based on the shortest period that provided a sufficient signal were used to estimate fragment abundance. The resulting IRMPD and CAD spectra are summarized in Table 1, and an example is shown in Figure 2 for protonated cefadroxil. For the comparison shown, the IRMPD spectrum is dominated by fragments at *m/z* 158 and 208, while the CAD spectrum shows a few other fragments because the collisional activation deposits a greater range of energies that results in less selective fragmentation.

Many of the dominant fragment ions formed were the same from both techniques, often involving cleavage across the β-lactam ring (see Scheme 1). For example, the dominant fragment ions in the PD spectrum of protonated cephalexin include ions at *m/z* 191 and 158, both of which are assigned structures in Scheme 1 and involve cleavage across the β-lactam ring. Kobayashi *et al.*[13] used HPLC/FABMS to analyze cephaloridine, cephalothin and cephalexin and 21 other cephem antibiotics, and many of the resulting fragment ions were the same as those obtained in our system. The IRMPD and CAD techniques also created similar numbers of fragments in terms of total abundance in the present work, although the IRMPD method often results in fewer types of fragments. Based on an estimation of how many of the precursor β-lactam ions are converted to fragment ions (i.e. dissociation efficiency) regardless of the activation time, the dissociation efficiencies of the

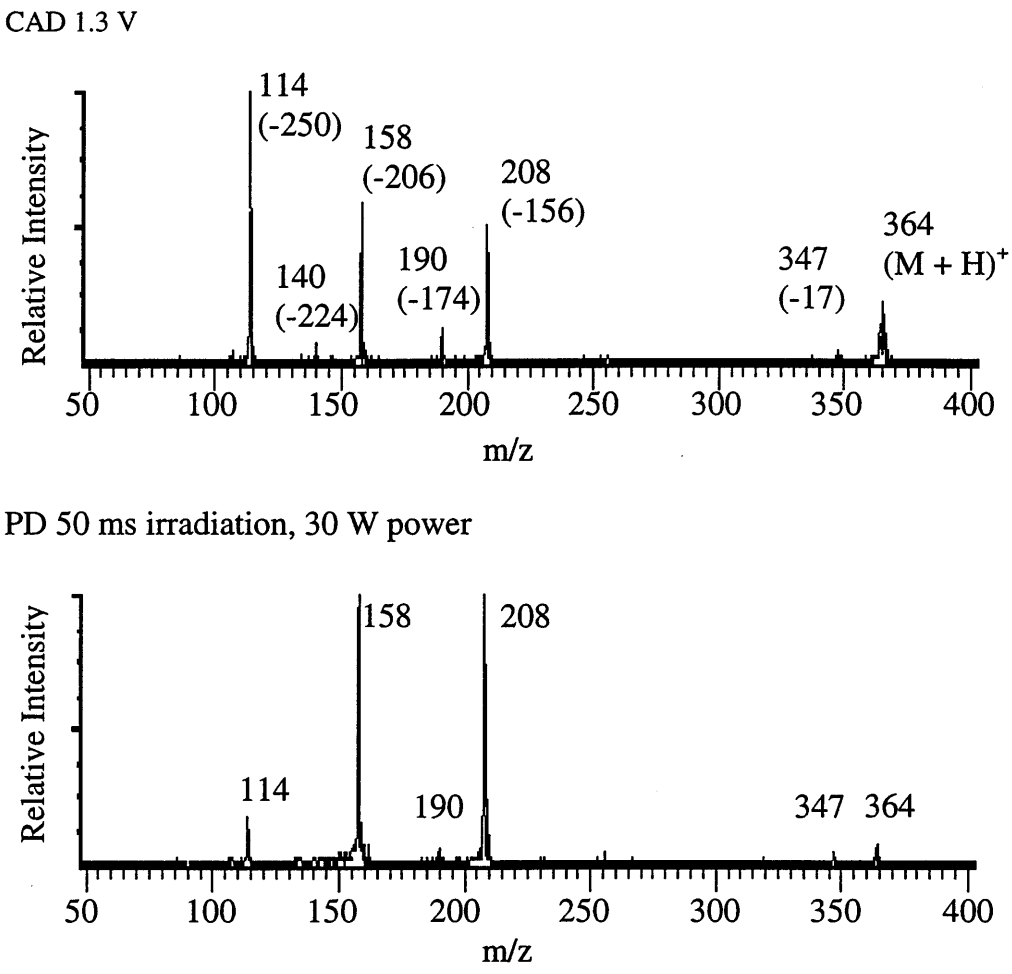

Figure 2. Dissociation of protonated Cefadroxil, *m/z* 364.

CAD and IRMPD methods are similar. IRMPD offers an advantage over CAD because PD does not require manipulation of the r.f. voltage to ensure trapping of kinetically energized ions. Hence the r.f. storage level may be lowered during the PD period without a decrease in activation efficiency or storage efficiency of higher mass ions. In many cases, use of low r.f. levels during CAD results in ineffective activation and poor

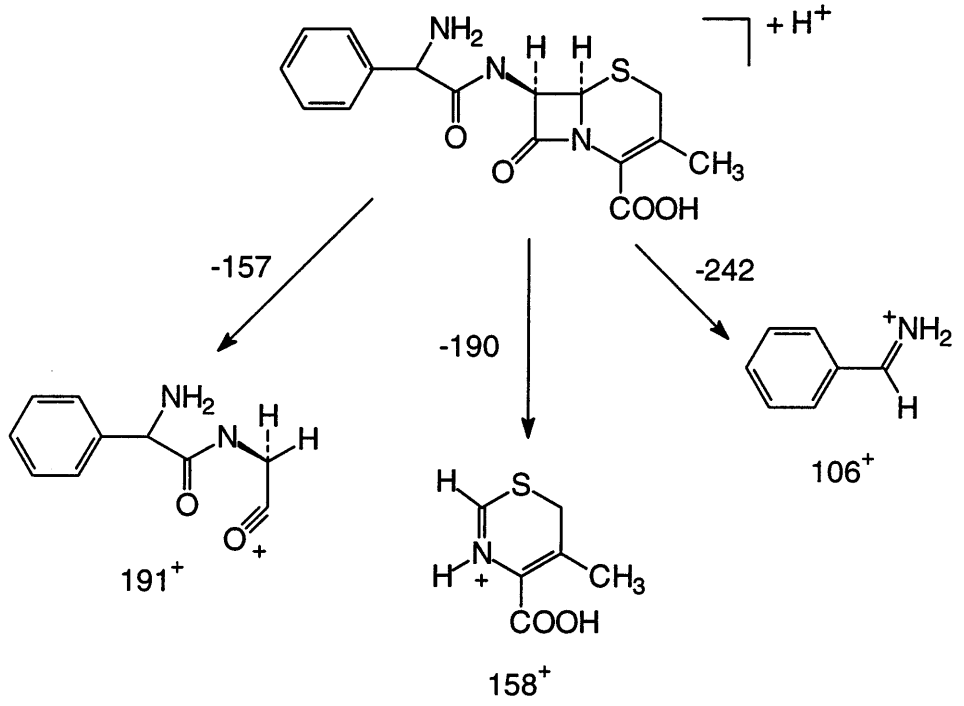

Scheme 1. Proposed fragmentation of protonated cephalexin, *m/z* 348.

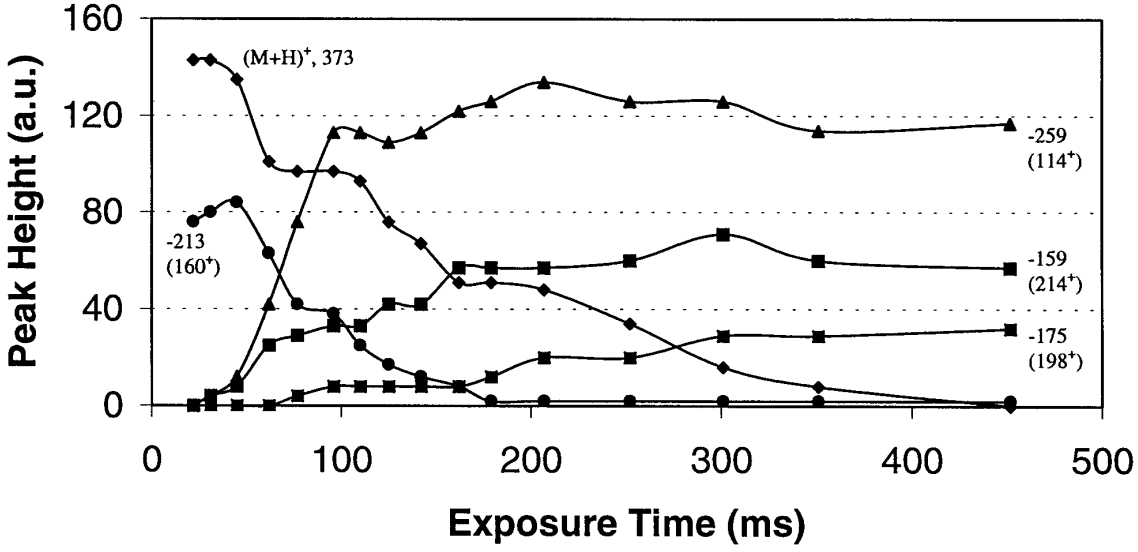

Figure 3. Time-resolved IRPD of [penicillin G, K salt + H]$^+$.

trapping efficiencies, as noted previously.[6] However, reasonably efficient CAD was achieved in the present study, even at low r.f. levels ($q_z = 0.13$). The fact that a compromise must often be made between efficiency of trapping and the low-mass cut-off is a disadvantage of CAD, especially for higher mass applications.

IR photons are absorbed by every organic analyte, thus causing photoactivation of all ions in the trap

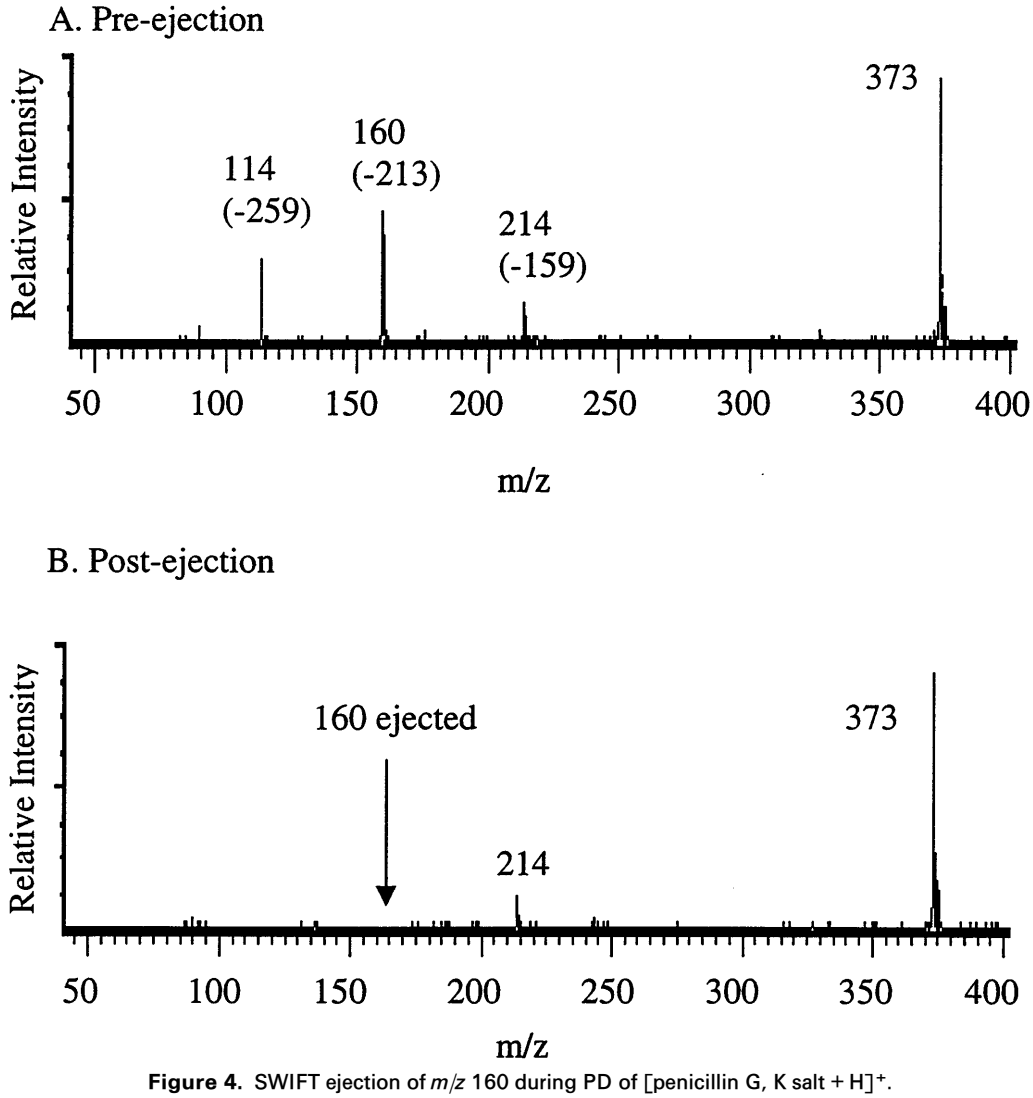

Figure 4. SWIFT ejection of m/z 160 during PD of [penicillin G, K salt + H]$^+$.

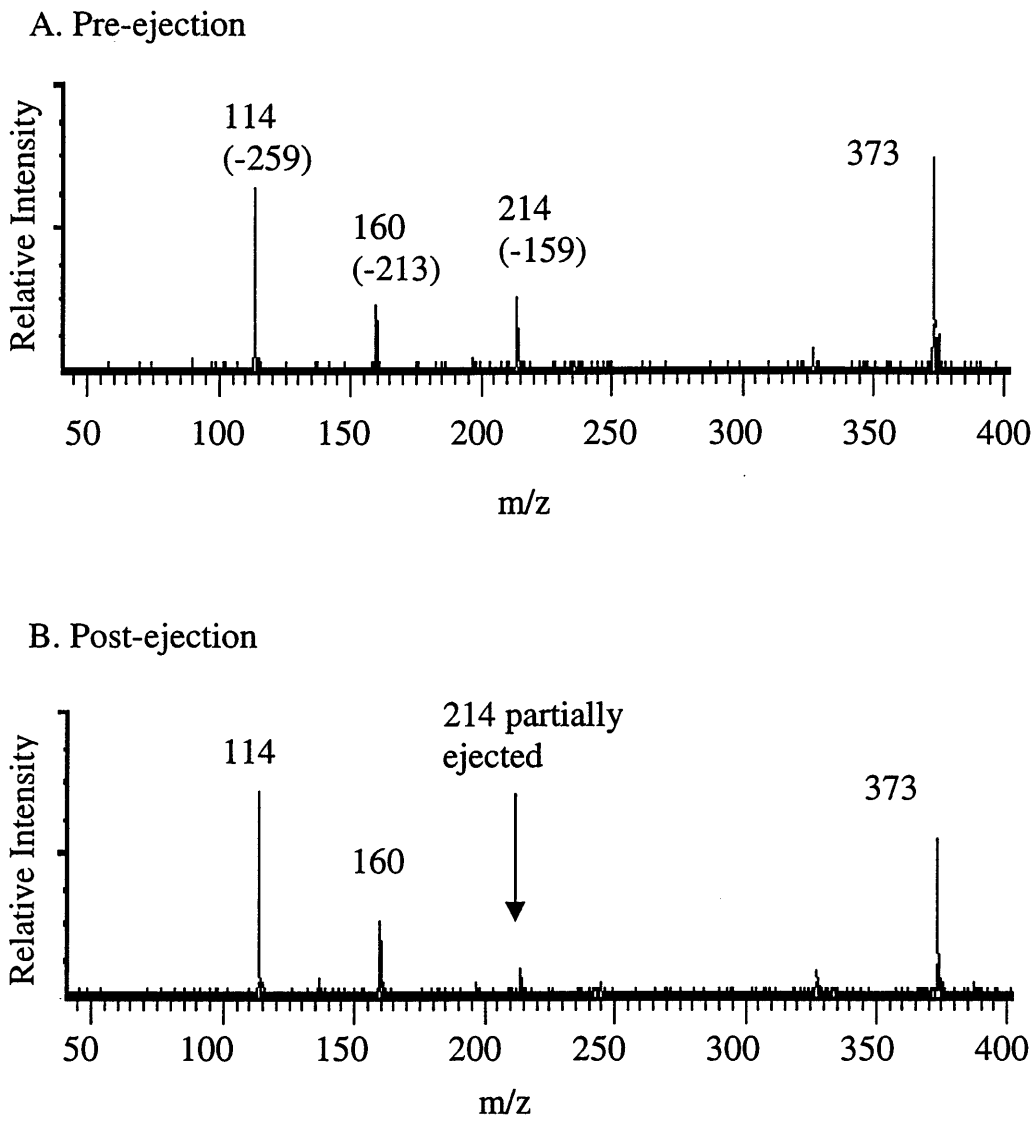

Figure 5. SWIFT ejection of *m/z* 214 during PD of [penicillin G, K salt + H]$^+$.

simultaneously. Like broadband CAD techniques such as boundary activated dissociation and off-resonance CAD,[18–21] the non-selectivity of IRMPD allows the rapid application of excitation energy without the necessity for fine tuning a mass or frequency setting. Furthermore, IRMPD applies relatively high energy over a broad mass range continuously, without the need to sweep through the mass range. This feature can be very useful when ion signals are transient or low level because fine tuning of the activation conditions is not needed, unlike in typical CAD experiments. Additionally, the non-selectivity can lead to excitation of primary fragments to produce additional fragments if PD is applied for a longer duration. This process can be useful for carrying out MS/MS/MS experiments, but the possibility of doing so unknowingly also exists. This latter factor may lead to some confusion about which fragment belongs to which precursor or which fragments stem from the secondary dissociation of other fragment ions.

The genealogy issue in PD has two solutions. One technique involves collecting time-resolved PD spectra. The irradiation time may be raised from 10 to 500 ms in 10–50 ms increments and the peak intensities recorded. Subsequently, an 'appearance/disappearance' plot can be made, showing which peaks appear as others disappear. Figure 3 is an example of such a plot, created using spectral data obtained from photodissociation of a protonated penicillin G–potassium complex. The first fragment to appear, representing a loss of 213 u, diminishes as three other fragments increase in abundance. Careful inspection of the time-resolved plot shows that the dominant reduction in the fragment due to loss of 213 u (formation of *m/z* 160 ion) coincides with the growth of the fragment due to loss of 259 u (formation of *m/z* 114 ion). The mass difference between *m/z* 160 and 114 is 46 u, a net difference that corresponds to HCOOH. The loss of 46 u from *m/z* 160 is easily rationalized:

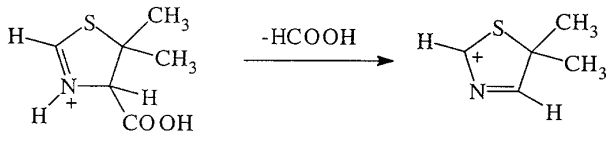

m/z 160 *m/z* 114

The resulting secondary fragment ion at m/z 114 may be further stabilized via resonance interactions involving the nitrogen and sulfur atoms. While m/z 214 and 198 ions appear as the m/z 160 ion become depleted, the fact that they are higher mass fragments indicate that they stem directly from the $[M + H]^+$ ion. In addition, the time-resolved plot gives further evidence that m/z 114 ion is formed only through primary formation of the m/z 160 ion. The abundance of the m/z 114 ion increases until the m/z 160 ion is thoroughly depleted, indicating that this pathway dominates the formation of the m/z 114 ion. As the irradiation time increases, conversion of m/z 160 to 114 may occur at a faster rate than the formation of m/z 160, so no m/z 160 peak appears in the spectrum. Hence the final abundance of m/z 114 is greater than the initial abundance of m/z 160.

This method requires a longer data acquisition time but clearly illustrates the trends in ion formation sequences. By optimization of the irradiation time, selective tailoring of the PD spectra can be undertaken to enhance the formation of secondary ions or to minimize sequential dissociation. Another technique for probing ion genealogy is by application of SWIFT waveforms for double resonance experiments. Using a SWIFT apparatus, a small frequency 'notch' can be used to eject one or more fragment ions at a time. If the targeted fragment ion is a precursor to any other fragment ions, then the secondary fragment ions also disappear. The SWIFT method allows the rapid determination of fragment ion genealogies.

For example, two SWIFT ejection experiments are illustrated in Figs 4 and 5. One shows a positive genealogical relationship and the other shows no relationship. Figure 4(A) illustrates the IRMPD spectrum of the protonated penicillin G–potassium salt with three major fragments. In Fig. 4(B), the fragment at m/z 160 is ejected simultaneously with irradiation, and the fragment at m/z 114 is no longer visible. Hence a positive genealogical relationship is confirmed between the ion at m/z 160 and the lower fragment ion at m/z 114. In contrast, Fig. 5 shows another SWIFT ejection experiment involving the protonated penicillin G–potassium salt in which partial ejection of the highest mass fragment ion (m/z 214) has little effect on the lower mass fragment ions (m/z 160 and 114), as predicted by the time-resolved PD plot. Such SWIFT experiments are easy to implement and ensure confident interpretation of fragmentation sequences.

In some cases, IRMPD gives fewer fragments of substantial ion current. Because of the low energy transferred by each photon, the excitation occurs in a stepwise manner. This results in the lowest energy dissociation pathway being accessed first. The presence of just one or two abundant fragments may indicate that the lowest energy dissociation pathway is dominant. For example, the amoxicillin and cephradine IRMPD spectra are extreme cases where only one major fragment is formed. This difference is also reflected in Fig. 2, in which cefadroxil has two dominant fragments under PD conditions, whereas CAD results in three major fragments.

CONCLUSIONS

Because gentle ionization and collisional cooling lead to ions with low internal energies in the ion trap, this setting is ideal for comparing energy deposition by various dissociation techniques. The infrared photoactivation process occurs by small, uniform increments that may lead collectively to a low or high energy deposition depending on the total time an ion spends in the path of the laser beam, whereas each collision in the CAD process may lead to a wide range of energy deposition depending on the initial position and exact frequency of the ion. Both processes are multi-step activation sequences and lead to a range of energy depositions in the ion trap. The differences in energy deposition account for the differences in the dissociation spectra. The non-selectivity of IR photoabsorption makes IRMPD universal while avoiding the pitfalls of frequency-specific activation techniques that add a dimension of difficulty to on-line studies. Most of the compounds in this study photodissociated by cleavage of the β-lactam ring. This result is consistent with the results of other studies.

IRMPD has been shown to be successful even in the higher pressure environment that results from residual solvent and atmospheric gases entering the vacuum chamber. Thus, the elevated pressures stemming from the ESI interface do not quench the photoactivation process and may assist in focusing the ions to the center of the trap where there is better overlap with the laser beam.[6] Moreover, the universal activation provided by IRMPD should be especially useful for LC/MS applications in which the masses and structural types of components in a complex mixture may vary dramatically and in which the time frame for isolation, optimization and dissociation of the eluting components does not permit the use of CAD methods.

Acknowledgements

The authors gratefully acknowledge financial support from the National Science Foundation (grant Nos CHE-9357422 and CHE-9421447), the Robert A. Welch Foundation (grant No. F1155), the Texas Advanced Research Program and the Dreyfus Foundation.

REFERENCES

1. J. L. Stephenson, Jr, M. M. Booth, S. M. Boue, J. R. Eyler and R. A. Yost, in *Biochemical and Biotechnological Applications of Electrospray Ionization Mass Spectrometry*, edited by P. A. Snyder, p. 513. American Chemical Society, Washington, DC (1996).
2. M. Gross, *Acc. Chem. Res.* **27**, 361 (1994).
3. R. Dongre, A. Somogyi and V. H. Wysocki, *J. Mass Spectrom.* **31**, 339 (1996).
4. P. Little, J. P. Speir, M. W. Senko, P. B. O'Connor and F. W. McLafferty, *Anal. Chem.* **66**, 2809 (1994).

5. M. E. Gimon-Kinsel, G. R. Kinsel, R. D. Edmondson and D. H. Russell, *J. Am. Soc. Mass Spectrom.* **6**, 578 (1995).
6. A. Colorado, J. X. Shen, V. H. Vartanian and J. S. Brodbelt, *Anal. Chem.* **68**, 4033 (1996).
7. R. Martin, in *Wilson and Gisvold's Textbook of Organic Medicinal and Pharmaceutical Chemistry*, edited by J. N. Delgado and W. A. Remers, 9th edn, Chapt. 7. J. B. Lippincott, Philadelphia, PA (1991).
8. M. S. Manhas and A. K. Bose, *Synthesis of Penicillin, Cephalosporin C and Analogs*, p. 25. Marcel Dekker, New York (1969).
9. L. A. Mitscher, H. D. H. Showalter, K. Shirahata and R. L. Foltz, *J. Antibiot.* **28**, 668 (1975).
10. M. D. Muller, J. Seibl and W. Simon, *Anal. Chim. Acta* **100**, 263 (1978).
11. S. Suwanrumpha, D. A. Flory, R. B. Freas and M. L. Vestal, *Biomed. Environ. Mass Spectrom.* **16**, 381 (1988).
12. Y. Shida and K. O'Hara, in *Proceedings of the 40th ASMS Conference on Mass Spectrometry and Allied Topics*, p. 1353, Washington, DC (1992).
13. K. Kobayashi, K. Sato, Y. Mizuno and Y. Katsumata, *J. Chromatogr. B.* **677**, 275 (1996).
14. M. Scandola, G. Tarzia, G. Gaviraghi, D. Chiarello and P. Traldi, *Biomed. Environ. Mass Spectrom.* **18**, 851 (1989).
15. A. F. Casy, C. Cryer and E. M. A. Ominde, *J. Pharm. Biomed. Anal.* **7**, 1121 (1989).
16. M. P. Barbalas, F. W. McLafferty and J. L. Occolowitz, *Biomed. Mass Spectrom.* **10**, 258 (1983).
17. G. J. Van Berkel, G. L. Glish and S. A. McLuckey, *Anal. Chem.* **62**, 1284 (1990).
18. S. A. Lammert and R. G. Cooks, *J. Am. Soc. Mass Spectrom.* **2**, 487 (1991).
19. M. Wang, S. Schachterle and G. Wells, *J. Am. Soc. Mass Spectrom.* **7**, 668 (1996).
20. J. Qin and B. Chait, *Anal. Chem.* **68**, 2108 (1996).
21. C. Paradisi, J. F. J. Todd, P. Traldi and U. Vettori, *Org. Mass Spectrom.* **27**, 251 (1992).

